

Performance analysis of continuous resource model updating in lignite production

Yüksel, Cansin; Benndorf, Jörg

DOI

[10.1007/978-3-319-46819-8_29](https://doi.org/10.1007/978-3-319-46819-8_29)

Publication date

2017

Document Version

Final published version

Published in

Geostatistics Valencia 2016

Citation (APA)

Yüksel, C., & Benndorf, J. (2017). Performance analysis of continuous resource model updating in lignite production. In J. J. Gomez-Hernandez, M. E. Rodrigo-Clavero, J. A. Vargas-Guzman, J. Rodrigo-Illari, & E. Cassiraga (Eds.), *Geostatistics Valencia 2016: 10th International Geostatistical Congress* (pp. 431-446). (Quantitative Geology and Geostatistics, QGAG; Vol. 19). Springer. https://doi.org/10.1007/978-3-319-46819-8_29

Important note

To cite this publication, please use the final published version (if applicable).
Please check the document version above.

Copyright

Other than for strictly personal use, it is not permitted to download, forward or distribute the text or part of it, without the consent of the author(s) and/or copyright holder(s), unless the work is under an open content license such as Creative Commons.

Takedown policy

Please contact us and provide details if you believe this document breaches copyrights.
We will remove access to the work immediately and investigate your claim.

Performance Analysis of Continuous Resource Model Updating in Lignite Production

Cansın Yüksel and Jörg Benndorf

Abstract Recently an efficient updating framework was proposed aiming to improve the raw material quality control and process efficiency in any type of mining operation. The concept integrates sensor data measured on the production line into the resource model and continuously provides locally more accurate resource models. A demonstration in lignite production is applied in order to identify the impurities (marine and fluvial sands) in the coal seams to lead better coal quality management. The updating algorithm applies different algorithmic parameters. This study aims to investigate the sensitivity of the performance with respect to different parameters for optimal application. Main parameters include the ensemble size, the localization and neighborhood strategies, and the sensor precision. The results should assist in future applications by determining the impact of the different parameters.

1 Introduction

One of the main challenges in lignite mining, similar to other branches of mining, is the waste intrusions in lignite seams. These marine and fluvial sand impurities can lead to high ash values (e.g., more than 15 % ash) and cannot be localized completely by exploration data and captured in the predicted deposit models.

Utilizing online sensor techniques for coal quality characterization in combination with rapid resource model updating, a faster reaction to the unexpected

C. Yüksel (✉)

Resource Engineering Section, Department of Geoscience & Engineering, Delft University of Technology, Stevinweg 1, 2628 CN Delft, Netherlands

e-mail: C.Yuksel@tudelft.nl

J. Benndorf

Institute for Mine Surveying and Geodesy, Faculty of Geosciences, Geoengineering and Mining, University of Technology Bergakademie Freiberg, Reiche Zeche, Fuchsmühlenweg 9, 09599 Freiberg, Germany

e-mail: J.Benndorf@tudelft.nl

deviations can be implemented during operations, leading to increased production efficiency. This concept was first proposed as a closed loop framework by Benndorf et al. (2015). The developed framework is based on ensemble Kalman filter (EnKF) and basically integrates the online sensor data into the resource model as soon as they are obtained.

The first investigation (Benndorf 2015) has proven the approach to work well within a synthetic case study under a variation of several control parameters (number of excavators, precision of the sensor, update interval, measurement interval, extraction mode/production rate). The second investigation (Wambeke and Benndorf 2015) introduced an extended version of the developed framework. This extension includes a Gaussian anamorphosis of grid nodes, sensor-based measurements, and model-based predictions; to deal with suboptimal conditions, an integrated parallel updating sequence; to reduce the statistical sampling error without the need of increasing the number of realizations and a neighborhood search strategy; to constrain computation time; and to avoid the spurious correlations. Thereafter, Yüksel et al. (2016) adapted the framework to update coal quality attributes in a continuous mining environment. The applicability of the framework for a full-scale lignite production environment is validated by successful results.

To further understand the effects of used parameters during the full-scale application, to identify the sensitivity of the results and explore the performance in depth, further studies are required. For this reason, this paper aims to investigate the performance of the resource model updating framework with respect to main parameters, which are the ensemble size, the localization and neighborhood strategies, and the sensor precision. Findings of this research are expected to assist in future applications of the resource model updating concept by making it easier to achieve optimum performance.

The remainder of the article is structured as follows: First, the ensemble Kalman Filter-based approach adapted to specific application in mining is briefly reviewed. Next, application in continuous mining test case is described, and sensitivity analysis experiments are described. Findings of the study are then presented. Key findings of the study are discussed and summarized. The article concludes with a summary of the research contributions and directions for the future research.

2 A Method for Updating Coal Attributes in a Resource Model Based on Online Sensor Data

For rapid updating of the resource model, sequentially observed data have to be integrated with prediction models in an efficient way. This is done by using sequential data assimilation methods, namely, the EnKF-based methods.

With the goal of a continuously updatable coal quality attributes in a resource model, a framework based on the normal-score ensemble Kalman filter (NS-EnKF) (Zhou et al. 2011) approach was tailored for large-scaled mining applications. The

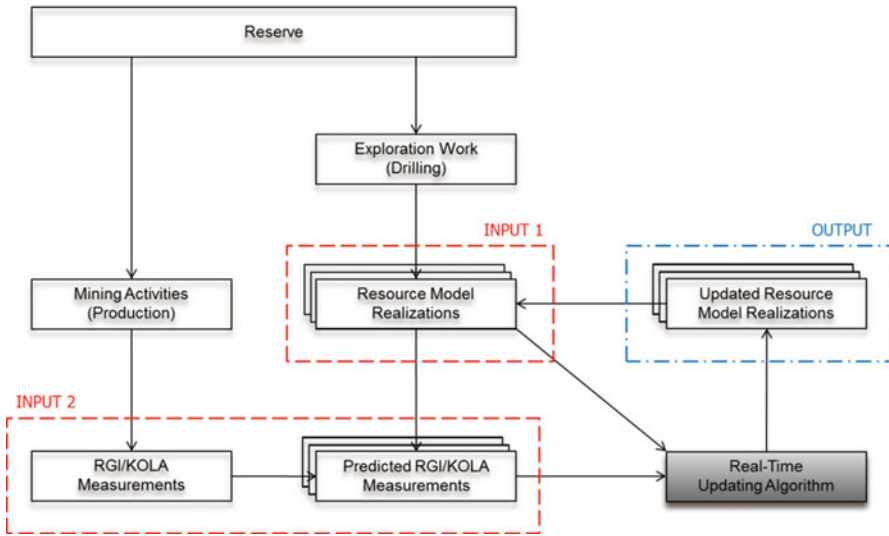


Fig. 1 Configuration of the real-time resource model updating concept (Modified from Wambeke and Benndorf 2015)

NS-EnKF is chosen to deal with the non-Gaussianity of the data by applying a normal-score transformation to each variable for all locations and all time steps, prior to performing the updating step in EnKF.

A formal description of the real-time updating algorithm is provided (Yüksel et al. 2016). Figure 1 gives general overview of the operations which are performed to apply the updating algorithm for improving the coal quality control using online data.

The concept initially starts with resource modeling by using geostatistical simulation technique, namely, sequential Gaussian simulation (SGS). This is the first required data set consisting of ensemble members to be updated. The second data set consists of a collection of actual and predicted sensor measurements. The actual online sensor measurement values are collected during the lignite production, and the predicted measurements are obtained by applying the production sequence as a forward predictor prior to resource model realizations. Once both of the input data are provided, the updated posterior resource model will be obtained. This process will continue as long as the online sensor measurement data is received.

3 Sensitivity Analysis on a Full-Scale Study

The aim of the case study presented here is to analyze the performance of the resource model updating framework method by performing sensitivity analyses on main parameters, including the ensemble size, the localization and neighborhood strategies, and the sensor precision.

3.1 *Identification of Main Parameters*

3.1.1 Number of Ensemble Members

The first sensitivity analyses focus on investigating the optimal realization number (subsequently used as ensemble size) by performing resource model updating experiments with different-sized ensembles. Defining the ensemble size that will fully represent the ore body is a very delicate problem. A lot of research in literature (Houtekamer and Mitchell 1998; Mitchell et al. 2002) focuses on the optimum ensemble size investigation and usually concludes that the analysis error decreases as the number of ensembles (realizations) increases. Contrary, the computational costs increase with the ensemble size. Therefore a sensible size of the ensemble is required.

3.1.2 Localization

The second sensitivity analyses focus on investigating the effects of localization strategies and neighborhood size on the given case. As mentioned, one of the limiting factors in EnKF-based applications is the restrained ensemble size. But having an insufficient ensemble size might cause long-range spurious correlations. In order to avoid these spurious correlations, a covariance localization technique is applied to the updating framework by Wambeke and Benndorf (2015). The spurious correlations refer to the correlations between quality attributes that are at a significant distance from one another where there is no spatial relation. Moreover, these correlations can lead to inbreeding and filter divergence. Covariance localization modifies update equations by replacing the model error covariance by its element-wise (the Schur) product with some distance-based correlation matrix (Gaspari and Cohn 1999; Horn and Johnson 1985). This replacement increases the rank of the modified covariance matrix and masks spurious correlations between distant state vector elements (Sakov and Bertino 2011).

3.1.3 Sensor Error

The final sensitivity analyses focus on testing the effect of the sensor precision. In most cases errors are involved when taking measurements, due to calibration issues of sensor technologies. For each experiment, different amounts of standard error are added to the actual measurement values. The standard error can be calculated as

$$SE_{\bar{x}} = \frac{\sigma}{\sqrt{n}} \quad (1)$$

where σ is the standard deviation of the actual measurements and n is the size (number of observations) of the actual measurements. For this study, the size of the actual measurement data set contains 700 observations, which values correspond to coal extracted from 28 mining blocks. This leads to approximately 25 actual measurement data per block. Therefore, where the added standard error is 0.1 % ash, the absolute standard deviation will be 0.5 % ash, and the variance will be 0.25 %² ash.

Similarly, when the added standard error is 0.2 % ash, the standard deviation will be 1 % ash, and the variance will be 1 %² ash. The variance of the actual measurements will be 6.25 %² ash, and the standard deviation will be 2.5 % ash when the added standard error is 0.5 % ash. The variance will be 25 %² ash when the added standard error is 1 % ash. The variance of the averaged prior model for 48 ensembles is calculated as 0.99.

To give a clear view, mentioned standard deviations are converted as the relative error of the measurements. The average measurement value is calculated as 12 % ash. This leads around 4 % ash relative error in measurement values when the added standard deviation is 0.5 % ash. Similarly, when the added standard deviation is 1 % ash, this indicates around 8 % ash relative error in measurement values. In the same way, when the added standard deviation is 2.5 % ash, this indicates around 20 % ash relative error in measurement values. Finally, when the added standard deviation is 5 % ash, this indicates around 40 % ash relative error in measurement values.

3.2 Experiment Setup

The case study is performed on a particular lignite seam in a mining operation in Germany. The seam contains multiple sand intrusions. The shape and size of these sand partings are irregular, and both characteristics are showing a large variability.

To apply the resource model updating algorithm, preparation of input data is required. First, the geological model of the defined coal seam is created on a 32 × 32 × 1 m dimensioned block model based on the roof and floor information of the lignite seam. Second, a 32 × 32 × 1 m dimensioned quality model capturing the wet ash content in percentages is generated with different number of simulations (24, 48, 96, 192, and 384), based on the provided drill hole data. The simulated ash

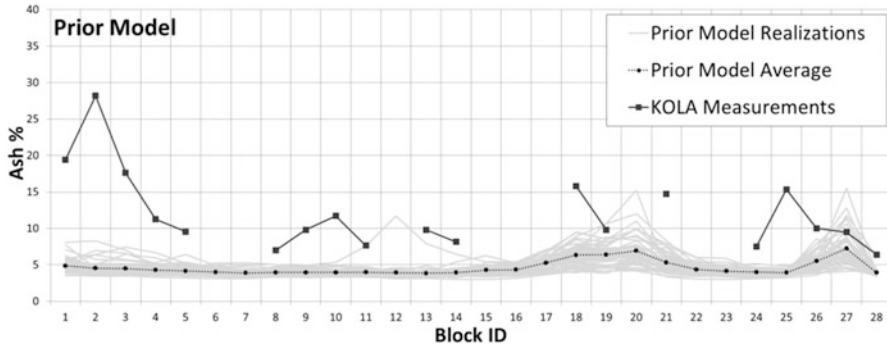


Fig. 2 Prior model and measurement data (before updating)

values are then merged with the previously defined coal seam. The block model realizations are now ready to be imported into the algorithm as the first input.

Figure 2 illustrates the prior model of 48 simulations, the averaged ash values of those simulations and related sensor measurement values, per block. A significant underestimation of the actual measurement data is observed in the prior model. This is because the prior model is created based on the drill hole data, where the local sand intrusions are not fully captured. True variability of the coal seam is captured by the online sensor measurements.

Predicted measurements are obtained by averaging the simulated ash values from each simulation set, which falls into the defined production block boundaries. The online sensor measurement data, namely, the Kohle OnLine Analytics (KOLA) data, are provided for the defined time period. KOLA system applies X-ray diffraction in order to accurately assess the components of the produced lignite. In order to determine the location of the received KOLA data, in other words to track back where the measured material comes from, the GPS data is matched with the measurement data based on the given timecodes. The located measurements in coal seam are then imported into the previously defined block model.

The second input file for the algorithm is written to a file containing the following information: the block ID, the central block location (X, Y, Z coordinates), and a series of real and predicted measurements.

A study bench is produced for a defined time period by considering all the available data (topography, RGI, GPS, and production data). Later, the study bench is divided into so-called production blocks. This was necessary to reproduce the excavated production blocks. The horizontal divisions (or production slices) are applied based on the movements of the excavator during production, provided by GPS data. The vertical divisions are based on the changes in the Z coordinates in the GPS data and capture a typical extraction sequence of bucket-wheel excavator operations. In total, the defined production bench is divided into 28 blocks and 5 slices, which gives 140 production blocks. Once the study bench is divided both in vertical and horizontal, the production blocks are now ready to be updated.

First the first block of the second slice will be updated, based on the KOLA measurements taken from that block. The series of updating experiments included seven updating experiments and continued until the ninth block (since there are no KOLA data obtained on sixth and seventh block, seven experiments are performed to update until the ninth block). In each updating experiment, only one block is updated based on the related measured KOLA value.

An empirical error measure so-called mean square difference or mean square error (MSE) is used in order to present results of the performed experiments. MSE compares the difference between estimated block value $\mathbf{Z}^*(x)$ and actual KOLA measurement \mathbf{v} values per block, and it can be calculated as

$$\text{MSE} = \frac{1}{N} \sum_{i=1}^N (\mathbf{z}^*(x_i) - \mathbf{v}_i)^2 \tag{2}$$

where $i = 1, \dots, N$ is the number of blocks. The mean square error graphs are calculated relative to the averaged prior model of 384 ensembles, in order to make a good comparison.

3.3 Experiments With Respect To Main Parameters

Table 1 provides a complete overview of the parameters used to perform the mentioned experiments. The obtained results of these experiments are provided in the next chapter. In every experiment performed for every parameter, one parameter is varied, and the others remain fixed (Table 1).

3.3.1 Number of Ensemble Members

With a view toward the real-time application of the updating resource model, the industrial case presented by Yüksel et al. (2016) focused on small- and moderate-sized ensembles (24). For the investigation of the optimum ensemble size, updating experiment series are performed with 24, 48, 96, 192, and 384 ensembles. All of the simulations are created by using SGS with same seed number and same variogram parameters.

3.3.2 Localization

The initial neighborhood size is defined as 450 m in X and Y directions and 6 m in Z direction based on the variogram of the drill hole data. For the experiments, three different neighborhood sizes (225, 450, and 900 m) are tested while the localization option was not being used. Three more experiments are performed while the localization option was being used in order to test the effect of designed

Table 1 Experimental schema

	Experiment #	Ensemble size	Localization option on/off and size (X,Y, Z) (m)	Neighborhood size (X,Y,Z) (m)	Relative sensor error (%)
Ensemble size experiments	1	24	On, 125,125,3	225,225,6	0
	2	48	On, 125,125,3	225,225,6	0
	3	96	On, 125,125,3	225,225,6	0
	4	192	On, 125,125,3	225,225,6	0
	5	384	On, 125,125,3	225,225,6	0
Localization and neighborhood strategies experiments	6	48	Off	225,225,6	0
	7	48	On, 225,225,3	450,450,6	0
	8	48	Off	450,450,6	0
	9	48	Off	900,900,6	0
	10	48	On, 450,450,3	900,900,6	0
	11	48	On, 450,450,6	900,900,6	0
Sensor error experiments	12	48	Off	450,450,6	4
	13	48	Off	450,450,6	8
	14	48	Off	450,450,6	20
	15	48	Off	450,450,6	40

localization, with varying localization and neighborhood sizes. For the experiments where the localization option was used, the localization neighborhood was assumed as half of the defined neighborhood size, except the tenth experiment. In the tenth experiment, in the X and Y direction, localization sizes were assumed as half of the defined neighborhood size. In the Z direction, the localization size remained the same. Reasons of this preference will be explained in the discussion chapter.

3.3.3 Sensor Error

For each experiment, different amounts of standard error are added to the actual KOLA measurement values. In total, five experiments are performed, where the relative measurement error varied between 4 %, 8 %, 20 %, and 40 %.

4 Results

4.1 Ensemble Size

Figures 3 and 4 present results of the updating process from the first block until the ninth block, for some of the representative ensemble sizes. For these experiment series, the localization strategies were applied; the neighborhood size was 225, 225, 6 m for X, Y, Z directions, respectively, and no sensor error is assumed.

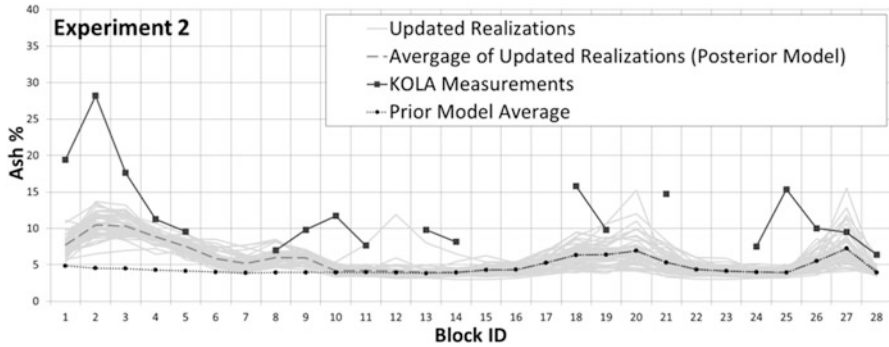


Fig. 3 Experiment 2 – ensemble size: 48

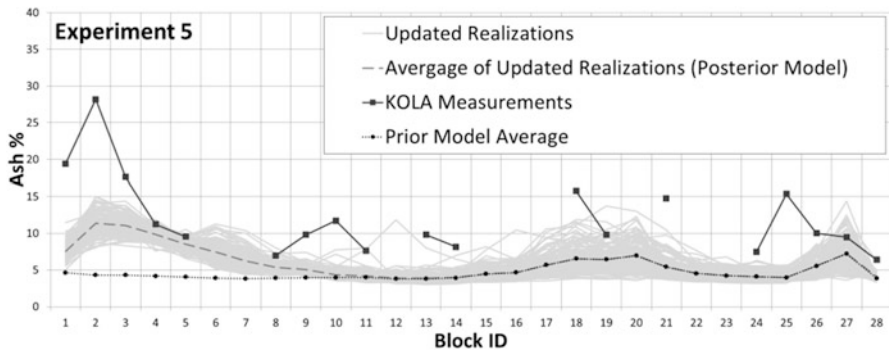


Fig. 4 Experiment 5 – ensemble size: 384

It can be seen that the average of the prior simulations substantially underestimates the actual KOLA measurements. This is caused by the data effect. The prior simulations are created based on the coal samples from drill holes spaced multiple hundred meters apart, while the KOLA measurements measure more higher ash values due to the sand intrusions in the coal seam. Integrating the KOLA measurement to the first nine blocks updates the neighborhood blocks to some relatively higher values. As expected, the update effect decreases while moving away from the last updated block, block 9.

For all different ensemble sizes, a clear improvement is observed toward the KOLA data when considering the average of the initial simulations, so-called prior model.

Figure 5 presents the relative MSE values to the prior model for each experiment performed with different ensemble sizes. The biggest reduction of the error occurs in the update of the first block. While the skewness behavior of each MSE graphs is similar, the biggest error behavior to the smallest is as follows: 48 ensembles, 96 ensembles, 192 ensembles, 384 ensembles, and 24 ensembles. Except for the results from 24 ensembles, the rest of the listing supports the literature. It is expected to observe a decrease in the MSE values while the ensemble size gets

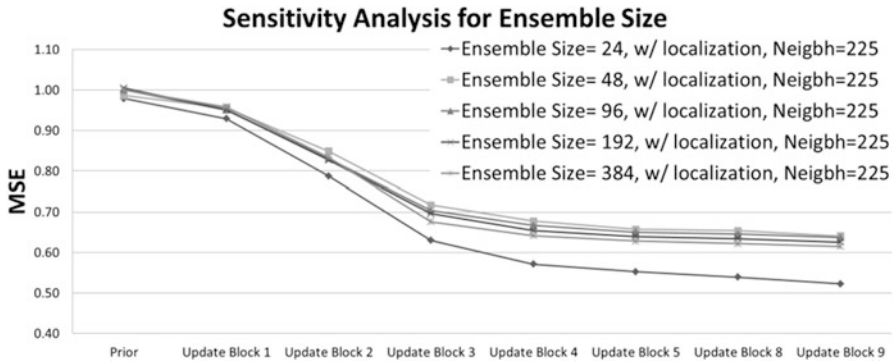


Fig. 5 Comparison graph for different ensemble-sized experiments

larger since the representativeness gets higher. However, to increase the computational efficiency and to apply the updating framework in real time during production, an economic ensemble size is required.

At first glance, higher initial variance of the 24 ensembles explains the very low MSE values. Nevertheless, a further investigation is performed in order to understand the phenomenon better. Five different sets of newly derived sets of 24 ensembles are generated with SGS, by using different random seeds for each set. New series of updating experiments are performed with the new series of 24 ensembles, and the results are compared. The comparison shows a high variety among results. MSE values obtained from the ninth block’s update varied between 0.52 and 0.69. In addition, the new sets of MSE values were equal to, lower or higher than the 48 ensembles, 96 ensembles, 192 ensembles, and 384 ensembles. This big variety, which is caused by different seed numbers, shows that 24 ensembles were not sufficient to represent a statistical stable estimate of the mentioned lignite seam.

When considering the 48 ensembles, even though the 48 ensembles have the highest MSE values by comparing to the 96 ensembles, 192 ensembles, and 384 ensembles, the MSE dropped from 1.0 to 0.64. In his research, Yin et al. (2015) found that improvements while using larger ensemble sizes (after the optimum ensemble size) are relatively insignificant. Likewise, the improvements between 48, 96, 192, and 384 ensembles are obvious, yet not very significant. For this reason, this study concludes that the optimal ensemble size for this specific study is 48 ensembles.

4.2 Localization and Neighborhood Strategies

Figures 6, 7, 8, and 9 present results of the updating process from the first block until the ninth block, for different localization strategies and neighborhood sizes. Experiments 2 (Fig. 3) and 6 (Fig. 6), Experiments 7 (Fig. 7) and 8 (Fig. 8), and

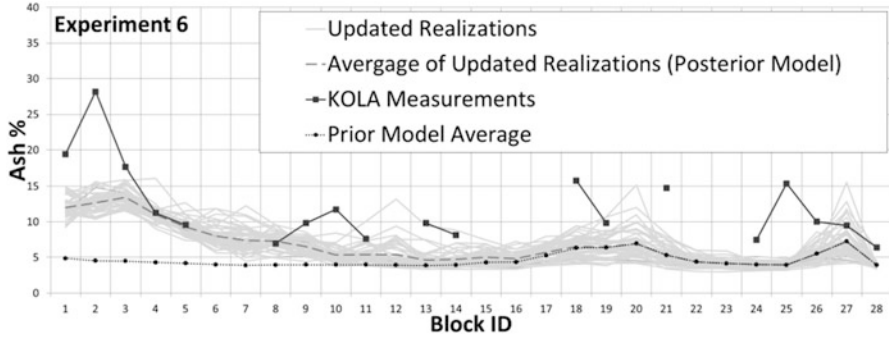


Fig. 6 Experiment 6 – localization option off, neighborhood size: 225, 225, 6 m

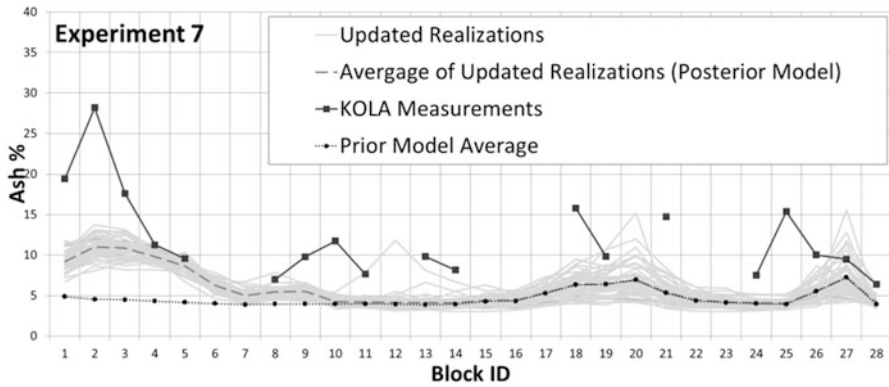


Fig. 7 Experiment 7 – localization option on (225,225,3 m), neighborhood size: 450, 450, 6 m

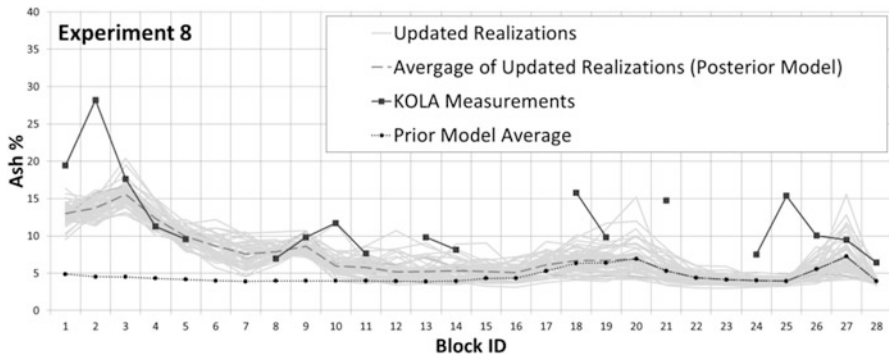


Fig. 8 Experiment 8 – localization option off, neighborhood size: 450, 450, 6 m

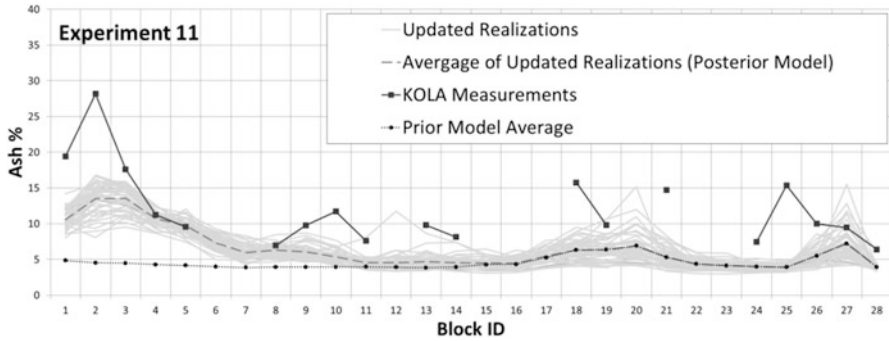


Fig. 9 Experiment 11 – localization option on (450,450,6 m), neighborhood size: 900, 900, 6 m

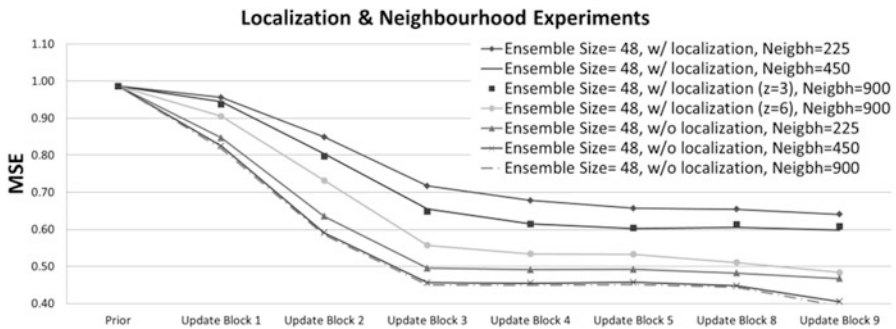


Fig. 10 Comparison graph for different localization and neighborhood strategies experiments

Experiments 9 (Fig. 9) and 10 (Fig. 10) are comparable to each other when investigating the localization option. Experiments 6 (Fig. 6), 8 (Fig. 8), and 9 are comparable to each other when investigating the neighborhood size.

Figure 10 compares all of the experiments performed in this section by plotting MSE values of each. Higher MSE values are observed when localization strategies are applied, and the neighborhood size is defined as 225, 225, 3 m. The MSE values become lower when the neighborhood size is increased and localization option is not used. This is expected because the neighborhood size was initially defined as 450, 450, 6 m based on the variogram, so performing the experiments with 225, 225, 3 m-sized neighborhood was not enough to cover the seam continuity. Minor changes are observed between the MSE values of 450, 450, 6 m neighborhood-sized experiment and 900, 900, 6 m-sized experiment due to no spatial correlation between the attributes.

The reason that applying the localization strategies did not provide any improvement in our case is due to the definition of the localization function.

Figure 14 illustrates the currently used function. Since the production block size is varying for each block, sometimes the plateau phase of the used function cannot cover a full block which is in the neighborhood. This creates un-updated values in a block and consequently the updating process of the entire block fails. For this

reason, better results are obtained while the localization strategies were not in use. The future study will improve this drawback by developing the localization function in a way that it can define the block boundaries and act according to those distances.

Experiment 10 uses the localization option with the following dimensions: 450, 450, 6 m in X, Y, Z directions. The used neighborhood size was 900, 900, 6 m. As mentioned before, the initial intention was to use a localization size half the size of the neighborhood size. Yet, since the depth of a production block is 6 m, limiting the localization by 3 m decreased the expected improvements. By running the same experiment, only changing the Z localization size parameter from 6 to 3 m, the same results as found in Experiment 6 (Fig. 6) are obtained. This can be observed in Fig. 10, by comparing the related MSE values.

4.3 Sensor Precision

Figures 11, 12, and 13 present the final results of the updating process from the first block until the ninth block, for different relative sensor errors. For all the experiments performed in this section, the average prediction quality gets better in the sense that they become closer to the KOLA measurement values.

When the relative sensor error gets higher, the posterior variance appears to increase significantly. This is mainly because the KOLA measurement values are almost out of the range of the prior model (Fig. 2), and the variance of the prior model significantly underestimates the KOLA measurement values. By integrating the KOLA measurements which have lower precision (applied relative error varies between 4 and 40 % ash), the algorithm opens up the option whether the KOLA data can be right or the prior model. Subsequently, this inflates the posterior uncertainty.

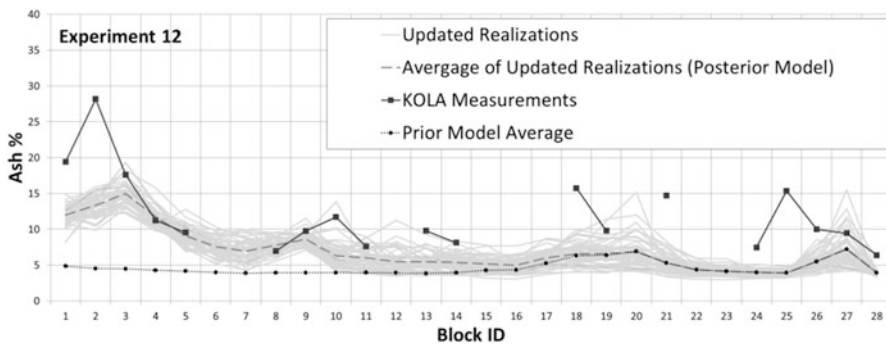


Fig. 11 Experiment 12 – relative sensor error: 4 %

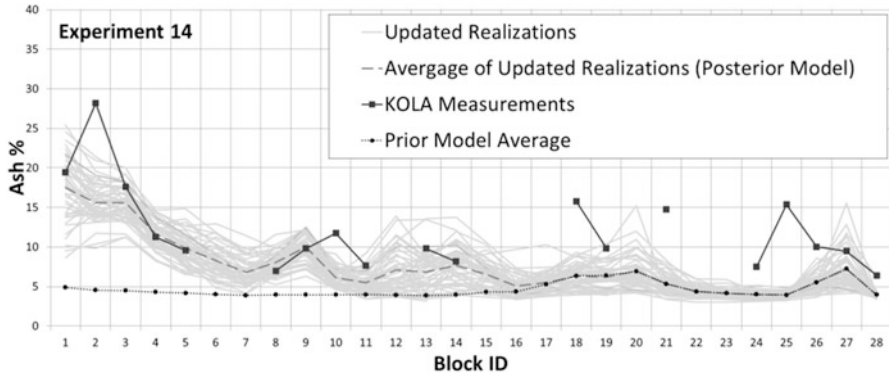


Fig. 12 Experiment 14 – relative sensor error: 20 %

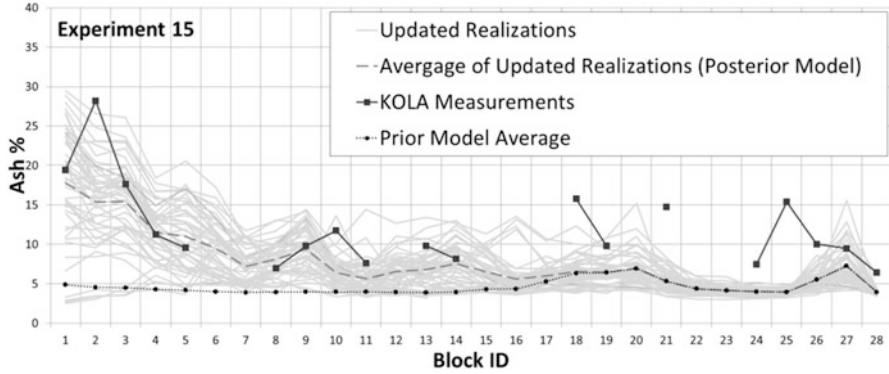


Fig. 13 Experiment 15 – relative sensor error: 40 %

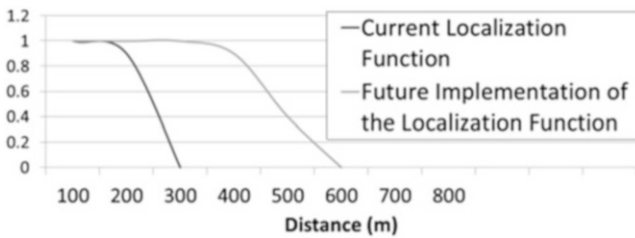


Fig. 14 Localization function illustrations

5 Conclusions and Future Work

This study analyzes the performance of the resource model updating method by performing sensitivity analyses on main parameters, including the ensemble size, the localization and neighborhood strategies, and the sensor precision in lignite

production. The results should assist in future applications by determining the impact of the different parameters.

The findings of ensemble size sensitivity analysis supported the existed literature (Houtekamer and Mitchell 1998; Mitchell et al. 2002), more accurate updates are achievable by using a bigger ensemble size. Although 24 ensembles provided the best results in terms of MSE, they are not chosen as the optimum ensemble size since they were not representative enough of the lignite seam. Instead 48 ensembles were, because it was the second best and was more representative of the lignite seam.

The sensitivity analyses of the localization and neighborhood strategies concluded that the applied localization strategies need to be improved, and the neighborhood size needs to remain as 450, 450, 6 m in X, Y, Z directions, as previously defined in the variogram modeling.

Sensitivity analyses for different sensor precision showed that the lower sensor precision increases the uncertainty of the posterior model, due to the significant difference between the prior model and the actual sensor data.

In general, the KOLA data is well covered by the range of uncertainty in the updated neighborhood. It is observed that the uncertainty in the near neighborhood gets slightly smaller and more of the actual KOLA measurements are captured by this uncertainty range.

The current research was limited to a case where only one excavator is operating. Future research should apply a case study where two, three, or four excavators are operating. This will require an update to the coal quality parameters in different production benches based on one combined material measurement.

Bibliography

- Benndorf J (2015) Making use of online production data: sequential updating of mineral resource models. *Math Geosci* 47(5):547–563
- Benndorf J, Yueksel C, Shishvan MS, Rosenberg H, Thielemann T, Mittmann R, Lohsträter O, Lindig M, Minnecker C, Donner R (2015) RTRO-coal: real-time resource-reconciliation and optimization for exploitation of coal deposits. *Minerals* 5(3):546–569
- Gaspari G, Cohn SE (1999) Construction of correlation functions in two and three dimensions. *Q J Roy Meteorol Soc* 125(554):723–757
- Horn RA, Johnson CR (1985) *Matrix analysis*. Cambridge University Press, Cambridge
- Houtekamer PL, Mitchell HL (1998) Data assimilation using an ensemble Kalman filter technique. *Mon Weather Rev* 126(3):796–811
- Mitchell HL, Houtekamer PL, Pellerin G (2002) Ensemble size, balance, and model-error representation in an ensemble Kalman filter*. *Mon Weather Rev* 130(11):2791–2808. doi:[10.1175/1520-0493\(2002\)130<2791:ESBAME>2.0.CO;2](https://doi.org/10.1175/1520-0493(2002)130<2791:ESBAME>2.0.CO;2)
- Sakov P, Bertino L (2011) Relation between two common localisation methods for the EnKF. *Comput Geosci* 15(2):225–237
- Wambeke T, Benndorf J. (2015) Data assimilation of sensor measurements to improve production forecasts in resource extraction. Paper presented at the IAMG, Freiberg (Saxony) Germany

- Yin J, Zhan X, Zheng Y, Hain CR, Liu J, Fang L (2015) Optimal ensemble size of ensemble Kalman filter in sequential soil moisture data assimilation. *Geophys Res Lett* 42 (16):6710–6715
- Yüksel C, Thielemann T, Wambeke T, Benndorf J (2016) Real-time resource model updating for improved coal quality control using online data. *Int J Coal Geol* 162:61–73, <http://dx.doi.org/10.1016/j.coal.2016.05.014>
- Zhou H, Gómez-Hernández JJ, Hendricks Franssen H-J, Li L (2011) An approach to handling non-Gaussianity of parameters and state variables in ensemble Kalman filtering. *Adv Water Resour* 34(7):844–864